2024 10th IEEE RAS/EMBS International Conference for
Biomedical Robotics and Biomechatronics (BioRob)
1-4 September 2024. Heidelberg, Germany

2024 10th IEEE RAS/EMBS International Conference for Biomedical Robotics and Biomechatronics (BioRob) | 979-8-3503-8652-3/24/$31.00 ©2024 IEEE | DOI: 10.1109/BIOROB60516.2024.10719949

Gaussian Process Regression Models for On-line Ankle Moment Estimation in Exoskeleton-Assisted Walking

Qingya Zhao, *Student Member, IEEE*, Rohan Deepak, Biruk A. Gebre, Karen J. Nolan, *Member, IEEE*
Kishore Pochiraju, *Member, IEEE*, and Damiano Zanotto*, *Member, IEEE*

***Abstract*— Ankle moment estimators inform the controllers of several assistive exoskeletons being developed in research labs. Accurate moment estimations are critical to ensure biomechanically relevant assistance. In this work, we propose new subject-agnostic ensemble Gaussian Process Regression (GPR) models which rely on a minimal set of in-shoe force and inertial sensors that do not require precise sensor-to-body alignment. We systematically analyzed the effects of model type, sensor set, and phase variable in terms of estimation accuracy by carrying out treadmill tests with 15 healthy individuals across a wide range of walking speeds. Our best ensemble GPR model achieved an average root-mean-square error of 3.6%±1.2% normalized over the gait cycle (equivalent to 8.8%±1.6% when normalized over the stance phase). Incorporating data from the inertial sensor and using the stance phase as the phase variable independently contributed to superior accuracy. Overall, these results indicate the potential of the proposed ensemble GPR models to accurately estimate ankle moments, paving the way for future applications to assistive powered ankle exoskeletons in real-world environments.**

***Index Terms*— Ankle Joint Moment Estimation, Gaussian Process Regression, Ankle Exoskeletons.**

I. INTRODUCTION

Lower-extremity trauma, neurological disorders, and age-related muscular degeneration often lead to reduced mobility, impacting the overall quality of life of affected individuals [1]. Given that the ankle plays a crucial role in stabilizing and propelling the body [2], powered ankle exoskeletons are among the most common lower-limb wearable robotic technologies proposed to enhance or restore ambulatory function. Most ankle exoskeletons designed for overground walking do not rely on a target trajectory [3]. Instead, locomotion assistance is provided based on torque templates [4], direct joint torque estimation [5], muscle activity amplification [6], or neuromuscular models [7], with the first two solutions being the most commonly adopted, owing to their robustness and ease of tuning [3]. Predefined torque assistance relies on a simplified torque template which is triggered at specific gait events [8], or provided as a continuous function of the gait phase [9]. Despite its robustness, this approach encounters challenges due to inter- and intra-subject differences and lack of adaptability to varying walking conditions. Direct joint torque estimation provides biomechanically relevant assistance by leveraging real-time approximations of the ankle's plantar- and dorsi-flexion (PDF) moment [10]. Ankle exoskeletons employing this control strategy capitalize on humans' natural optimization tendencies, wherein individuals adapt their walking patterns in response to environmental cues and task demands [11]. However, the efficacy of this method is contingent upon the accuracy of the ankle moment estimation model, and achieving high accuracy using only wearable sensors presents a significant challenge.

The methods proposed to date can be classified into *biomechanical models* and *regression-based approaches*. Choi *et al.* [12] employed a planar inverse-dynamics model to estimate ankle PDF moments. The model requires knowledge of the mass distribution of the foot and relies on measurements of the normal ground reaction forces (GRF), the anteroposterior projection of the foot center of pressure (COP), and the foot angular acceleration, which were obtained from underfoot pressure and inertial sensors. However, because it is impractical to estimate the foot anthropometric parameters for each individual, this method uses approximated normative data, which affects its accuracy. In the model developed by Bishe *et al.* [13] for an ankle exoskeleton, the ankle plantarflexion moment was obtained as the product of the normal GRF under the forefoot measured by a customized force-sensitive resistor (FSR) and the average tangential distance between the forefoot and the ankle joint, which was assumed to be a fixed parameter independent of gait phase, walking speed, or foot length. The estimator proposed by Gasparri *et al.* [10] for the same exoskeleton predicts the normalized plantarflexion moment by feeding the normalized sum of two forefoot FSR signals as input to a best-fit quadratic polynomial. The outputs of this model enable robust control of the exoskeleton under different walking conditions at the expense of biomechanical fidelity, since the estimator was trained solely on peak FSR-to-moment data from a single subject, neglecting both phase-dependent COP variations and inter-subject variability.

Owing to their extensive expressive capabilities, machine learning models have the potential to enhance the accuracy of ankle moment estimators, outperforming traditional parametric regression models. Jacobs *et al.* [14] used feed-forward neural networks (NN) to estimate the normalized ankle PDF moment from 8 custom underfoot pressure sensors and a miniature load-cell located on the Achilles tendon. While these models apply to both walking and calf rise tasks, they require subject-specific training, which reduces their range of applicability. Hossain *et al.* [15] introduced a subject-agnostic deep learning model, dubbed Kinetics-FM-DLR-Ensemble-Net, for estimating lower-extremity joint moments

*Corresponding author (dzanotto@stevens.edu).
QZ, RD, BAG, KP, and DZ are with the Dept. of Mechanical Engineering, Stevens Inst. of Technology, Hoboken, NJ 07030, USA. KJN is with Human Performance and Engineering Research, Kessler Foundation, West Orange, NJ 07052, USA and Rutgers-NJMS, Newark, NJ 07103, USA.

using three inertial measurement units (IMUs) attached to the thigh, shank, and foot. This work highlights the benefits of using ensemble learners in terms of model accuracy. However, their estimator was trained on a predefined set of treadmill speeds applied to all subjects, which may affect the generalization of their models. Other authors have proposed the use of electromyography (EMG) in their learning-based estimators. Ardestani *et al.* [16] employed a wavelet NN to reconstruct joint moments from 10 lower-body EMG signals and 2 GRF projections. While their method is subject- and task-agnostic and proved to be more accurate than feed-forward NN, it requires gait laboratory equipment. Xiong *et al.* [17] employed a traditional NN informed by 3 EMG signals and 5 joint angles from the lower extremities to reconstruct ankle PDF moments during walking. Although their approach is, in principle, applicable to wearable sensors, their models are not subject-agnostic. Grzesiak *et al.* [18] used an adaptive weighted Long Short-Term Memory (LSTM) ensemble network to predict ankle PDF moments in different locomotor tasks using time features extracted from 4 wireless EMG sensors with embedded three-axis accelerometers in each leg. Their results indicated that ensemble LSTM models outperform individual LSTM models, however, their models require subject-specific training. Leveraging the same sensor setup, Sloboda *et al.* [19] applied parameter-based transfer learning to train LSTM models for ankle moment estimation. However, their approach still requires labelled data from the target user. Recently, researchers have investigated the use of muscle ultrasound (US) imaging as an alternative noninvasive sensing mechanism for device control. Rabe *et al.* [20] estimated hip, knee, and ankle joint moments during treadmill walking through Gaussian process regression (GPR) models informed by a single US transducer located in the anterior thigh. In treadmill walking at different speeds, Zhang *et al.* [21] found that subject-specific convolutional neural networks (CNN) trained with signals from a single US transducer located on the calf muscles could outperform corresponding CNN models trained with signals from 3 EMG channels in the Gastrocnemius and Soleus muscles. Despite encouraging results, both Rabe's and Zhang's methods require subject-specific data to train the models.

In summary, previous research in ankle PDF moment estimation have relied on simplistic biomechanical models, traditional parametric regression, or machine learning models. However, to the best of the authors' knowledge, *no work to date has developed learning-based subject-agnostic models for ankle moment estimation that only require in-shoe wearable sensors.* Building on our previous study [22], we introduce new subject-agnostic GPR models for online ankle moment estimation that rely on a minimal set of affordable in-shoe sensors, namely an 8-cell array of FSRs and an IMU, which do not require precise sensor-to-body alignment, aside from the natural alignment provided by fitting the foot in the shoe. These attributes are critical to facilitate implementation on a powered orthosis. We evaluate the accuracy of these models with a group of healthy individuals during treadmill walking tests at different speeds. Additionally, we analyze the effects of model type (ensemble GPR vs. Least Absolute Shrinkage and Selection Operator, LASSO), sensor set (FSR vs. combined FSR+IMU) and phase variable (gait cycle – GC% vs. stance phase – ST% vs. no phase variable – NP) in terms of model accuracy. Finally, we perform a feature analysis to ascertain the relative importance of the input features extracted from the FSR and IMU sensors. The remainder of the paper is organized as follows: Section II describes the experimental protocol. Section III introduces the GPR models we applied to estimate the ankle moment, and Section IV summarizes the results of the study. Lastly, the paper is concluded in Section V.

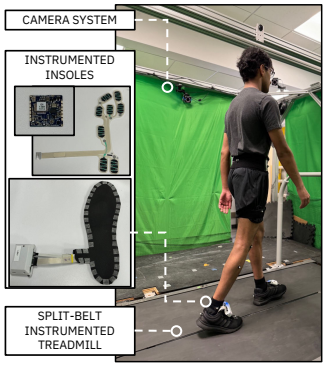

Fig. 1. Experimental setup. Features extracted from insoles instrumented with IMU and an 8-cell FSR sensor [23], [24] were used to inform the ankle moment estimator. An optical motion capture system and a split-belt treadmill served as reference systems.

II. EXPERIMENTAL PROTOCOL

Fifteen able-bodied individuals participated in this study (13 M, age 24.08 ± 4.97 years, height 1.72 ± 0.07 m, weight 72.12 ± 15.04 kg, comfortable walking speed (CWS) 1.02 ± 0.26 m/s). Prior to data collection, each participant selected an appropriate size of instrumented insoles among 8 available sizes, and fit them into their own shoes. The insole system, which features a 9-DOF IMU and a 8-cell array of FSRs, is a custom device developed by our group [23], [24]. This sensor configuration was selected for developing the ankle moment estimator owing to its minimal setup time and ease of integration with a portable ankle exoskeleton featuring external shoe brackets [25], [26]. An optical motion capture system with 9 cameras (Vicon Motion Systems, Oxford, U.K.) and a split-belt force-measuring treadmill (Bertec, Columbus, OH) were used to extract reference ankle PDF moments (Fig. 1). To this end, 16 reflective markers were placed on the participant's body, following the VICON Plug-in Gait lower body marker set. The participant was then instructed to complete a 10-minute familiarization session on the treadmill during which their comfortable walking speed was determined using the iterative procedure described in [27]. Afterwards, each study participant walked on the treadmill at 3 fixed speeds (CWS, 85% CWS, 115% CWS), for 3 minutes each, with 1-minute rests in-between bouts [28], Fig. 2. Marker and force-plate data were sampled at 100 Hz and 900 Hz, respectively. Insole data were stored in

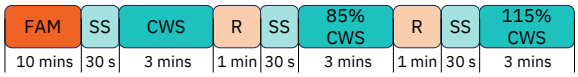

Fig. 2. Experimental protocol. FAM: familiarization bout, SS: standing still; R: resting; CWS: comfortable walking speed.

each insole's electronic pod, at a sampling rate of 333Hz. Synchronization between the reference equipment and the insole system was achieved through a custom wireless board [28]. The study was approved by the IRB of Stevens Institute of Technology, and all participants provided written informed consent.

III. METHODS

A. Data pre-processing

To ensure steady-state gait patterns, we considered only the last 30 seconds of each fixed-speed walking bout, for each participant. Marker positions were employed to scale the generic OpenSim musculoskeletal model to each participant, following which ground-truth ankle PDF moments were estimated from inverse dynamics [29]. Heel-strike (HS) and toe-off (TO) events were identified from force plate data using a fixed threshold algorithm with a 5% body weight threshold [14]. Subsequently, HS and TO events were used to segment FSR and IMU signals into gait cycles and stance phases. Based on preliminary tests, we considered the following candidate input features for the ankle estimator: all FSR signals from the 8-cell array, magnitudes of the acceleration and angular velocity vectors (a_M, g_M), vertical projection of the acceleration (a_Z), mediolateral projection of the angular velocity (g_X), and participant's shoe size (EU size). The latter was used as a surrogate measure for the participant's foot size. The eight FSR signals were scaled to the range $[0, 1]$ using the range of the FSR readings collected over the three fixed-speed walking bouts. Subsequently, all candidate input features were segmented into $N = 101$ equally spaced points (i.e., $[0\%, 100\%]$), either in the ST% domain or in the GC% domain (see Sec. III-C). Participants' shoe sizes were also normalized within the range $[0, 1]$.

B. Ankle Moment Estimators

Leave-one-out cross-validation (LOOCV) was used to train LASSO and GPR models, subject by subject, using data from all the other subjects (Fig. 3).

1) LASSO: These generalized linear models were introduced as a baseline to evaluate the extent to which the complexity of GPR models is justified by their enhanced accuracy. We trained N independent models with weights $\hat{\omega}_i$ given by

$$\hat{\omega}_i = \min_{\omega}(Y_i^{tr} - X_i^{tr}\omega)^T(Y_i^{tr} - X_i^{tr}\omega) + \lambda\|\omega\|_1,\ i \in [1, N], \quad (1)$$

where i indicates the phase index (GC% or ST%), λ is a non-negative regularization parameter, and Y_i^{tr}, X_i^{tr} are the reference ankle moment and the vector of input features in the training dataset at phase i. Vector X_i^{tr} was augmented with the constant 1 to account for the intercept, and the tuning parameter λ was chosen as the largest value resulting in a non-null model. For NP models, we set N≡1 in (1).

2) GPR: We regard the ankle moment estimation as the output of a noisy observation model

$$y = f(\boldsymbol{x}) + \epsilon, \quad (2)$$

where $\boldsymbol{x}$ is the input vector, y is the observed target value, $f(\boldsymbol{x})$ represents the latent function value with added Gaussian noise $\epsilon \sim \mathcal{N}(0, \sigma_n^2)$ and σ_n^2 is the noise variance of the n observations. A Gaussian process (GP) defines a distribution over functions with a mean function $m(\boldsymbol{x})$ and a covariance function $k(\boldsymbol{x}, \boldsymbol{x}')$ between two random variables $\boldsymbol{x}$ and $\boldsymbol{x}'$:

$$f(\boldsymbol{x}) \sim \mathcal{GP}(m(\boldsymbol{x}), k(\boldsymbol{x}, \boldsymbol{x}')). \quad (3)$$

In this work, the mean function $m(\boldsymbol{x})$ was chosen as a fixed constant function $\boldsymbol{H}\beta$, with $\boldsymbol{H}$ being a n_{tr}-by-1 basis vector of ones and β a coefficient inferred from the training data. Given n_{tr} training data points $X^{tr} = \{x_j\}_{j=1}^{n_{tr}}$ and corresponding response observations Y^{tr}, a GP predicts the latent values $\mathbf{f}_*$ for the n_{te} test points $X^{te} = \{x_j\}_{j=1}^{n_{te}}$ as

$$\mathbf{f}_*|X^{tr}, Y^{tr}, X^{te} \sim \mathcal{N}(\bar{\mathbf{f}}_*, \mathrm{cov}(\mathbf{f}_*)). \quad (4)$$

The covariance function defines the covariance matrices between the training data points $K \triangleq K(X^{tr}, X^{tr})$, test and training data points $K_* \triangleq K(X^{te}, X^{tr})$, and the test data points $K_{**} \triangleq K(X^{te}, X^{te})$. The optimal hyperparameter set $\boldsymbol{\theta}$ and β are optimized from the training data to maximize the marginal log-likelihood function

$$\begin{aligned}\log p(Y^{tr}|X^{tr}, \beta, \boldsymbol{\theta}) = \\ -\frac{1}{2}(Y^{tr} - \boldsymbol{H}\beta)^T(K + \sigma_n^2 I)^{-1}(Y^{tr} - \boldsymbol{H}\beta) \\ -\frac{1}{2}\log|K + \sigma_n^2 I| - \frac{n}{2}\log 2\pi\end{aligned} \quad (5)$$

To this end, we use the Symmetric Rank 1 (SR1) quasi-Newton gradient method [30]. The predictive mean and covariance for new test data points are then calculated as

$$\bar{\mathbf{f}}_* = \boldsymbol{H}_*\beta + K_*^T(K + \sigma_n^2 I)^{-1}(Y^{tr} - \boldsymbol{H}\beta), \quad (6)$$

$$\mathrm{cov}(\mathbf{f}_*) = K_{**} - K_*^T(K + \sigma_n^2 I)^{-1}K_*, \quad (7)$$

where $\boldsymbol{H}_*$ is an n_{te}-by-1 vector of ones and $\bar{\mathbf{f}}_*$ is the expected value of the estimations Y^{te} for the test data points.

A Genetic Algorithm (GA), was employed as a wrapper method to determine the optimal subset of input features I_{opt} and the optimal covariance function k_{opt} for the GPR models. To this end, we implemented a nested 10-fold cross-validation loop within the LOOCV (Fig. 3), using the average mean absolute error (MAE) across the 10 folds as the GA cost function. The candidate input features comprised those outlined in Sec. III-A. For GC% and ST% models, we included the phase index i as an additional input. To expedite the feature selection process, we grouped the eight FSR signals into four categories: *Heel* (encompassing medial and lateral heel FSRs), *Arch* (represented by the mid-foot FSR), *Met* (including the 1st, 3rd, and 5th metatarsal FSRs), and Toes (encompassing the hallux and toe FSRs). This grouping ensured that all FSR signals within a group would either be retained or discarded together. Based on preliminary tests, we restricted the candidate covariance functions for GPR to exponential, exponential with automatic relevance determination (ARD), Matérn kernel $3/2$ with ARD, Matérn kernel $5/2$ with ARD, and rational quadratic with ARD [31].

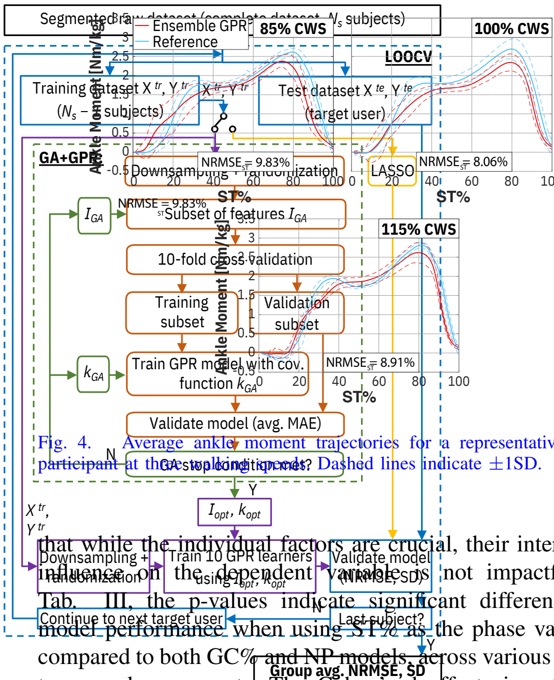

Fig. 3. Framework to train/test subject-agnostic ankle moment estimators based on ensemble GPR. The LASSO model is included for comparison and is not part of the proposed method.

Fig. 4. Average ankle moment trajectories for a representative study participant at three walking speeds. Dashed lines indicate ±1SD.

Within each LOOCV iteration, we trained 10 GPR models using I_{opt} and k_{opt} and regarded the average prediction from these 10 models as the output of an ensemble GPR learner. Considering the computational complexity of GPR is $O(n^3)$, we reduced the number of observations in the LOOCV training dataset X^{tr}, Y^{tr} by decimating the samples within each stride by a factor of 2 and by randomly selecting one complete stride from each of the ($N_s - 1$) participants for each speed. To generate 10 training datasets for the ensemble learner we repeated this random stride selection 10 times, without replacement.

To quantify the accuracy of the ensemble GPR and LASSO models, we used the normalized root-mean-square errors computed over stance-phase data ($NRMSE_{ST}$). This was done to ensure a fair comparison between models based on GC% and those based on ST% (see Sec. [illegible]). Specifically, for each LOOCV iteration, $NRMSE_{ST}$ was computed by dividing the RMSE of all model predictions on the test dataset by the range of ankle moment observed in the same dataset. All models were evaluated on the complete test set X^{te}, Y^{te} (i.e., no downsampling or random stride selection was applied). Model training and testing were conducted on a 2.3 GHz Intel® Core™ i7-11800H using MATLAB (The Mathworks Inc., Natick, MA).

C. Data Analysis

A 3-way repeated-measures ANOVA was used to identify significant ($\alpha = 0.05$) effects of *model type – M* (LASSO vs. ensemble GPR), *sensor set – S* (FSR vs. combined FSR+IMU), and *phase variable – P* (GC% vs. ST% vs. NP) on prediction accuracy. Post-hoc analyses were carried out where appropriate, using Bonferroni-Holm correction.

TABLE I

p-VALUES OF THE 3-WAY REPEATED-MEASURES ANOVA.

	M	S	P	M*S	M*P	P*S	M*S*P
p	< 0.001	< 0.001	< 0.001	0.407	0.291	0.122	0.187
Cohen's f	0.895	1.024	0.959	0.229	0.339	0.337	0.366

M: Model type; S: Sensor set; P: Phase variable;

TABLE II

p-VALUES OF THE POST-HOC ANALYSIS FOR PHASE VARIABLE.

	ST%–GC%	ST%–NP	GC%–NP
p	0.002	< 0.001	0.094
Cohen's d	0.985	1.272	0.464

Effect sizes for the three ANOVA factors and for the post-hoc analyses were evaluated using Cohen's f and Cohen's d, respectively. Additionally, feature selection ratios[1] were computed for each candidate input feature in the GA-optimized GPR models to evaluate the relative importance of each feature. This analysis was carried out using SPSS v29 (IBM Corporation, Armonk, NY).

IV. RESULTS

A total of 1125 strides were extracted from the instrumented insoles. Participants' walking speed varied from 0.54 m/s to 1.56 m/s. Fig. 4 shows the ankle moment of the left foot estimated with an ensemble GPR model using combined FSR+IMU inputs and ST% as the phase variable. Fig. 5(a) shows the group averages of $NRMSE_{ST}$ for all combinations of model type, sensor set, and phase variable, while Tab. I and Tab. II summarize the results of the 3-way ANOVA. GPR models outperformed LASSO models, independently of the sensor set or phase variable. Moreover, the addition of IMU-derived signals significantly improved the accuracy of the estimations, independently of the model type. The use of ST% as the phase variable significantly improved the estimation accuracy compared to both GC% and NP models, regardless of the model type and sensor set. However, there was no significant difference between GC% and NP models. Notably, effect sizes were very large for all significant factors and pairwise comparisons, indicating strong influences on model accuracy. Fig. 5(b) shows the selection ratio of each candidate feature for different sensor sets and phase variables. The most recurrent features in the optimized GPR models were the FSRs underneath the calcaneous and metatarsal heads, along with the normalized shoe size (selection ratio ≥ 0.93). When IMU data were available to train the models and a phase variable was included in the feature set, the magnitude of the foot acceleration a_M was also a recurrent feature (selection ratio ≥ 0.80), while data from the gyroscope appeared to contribute less (selection ratio ≤ 0.27). For GPR models that did not rely on a phase variable, all inertial signals except g_z appeared to be moderately important (selection ratio ≥ 0.47).

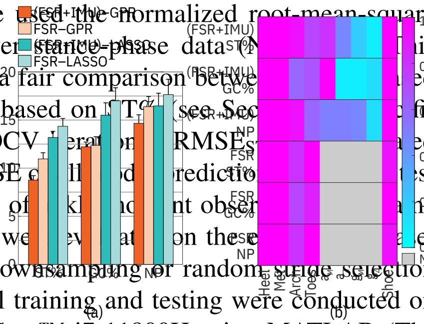

Fig. 5. (a) Group averages of the $NRMSE_{ST}$ for the ankle moment estimators. Error bars indicate +1SE. (b) Selection ratio of the input features for the optimized ensemble GPR models.

that while the individual factors are crucial, their interactive influence on the dependent variables is not impactful. In Tab. III, the p-values indicate significant differences in model performance when using ST% as the phase variable, compared to both GC% and NP models, across various model types and sensor sets. The Cohen's d effect sizes further reveal that incorporating ST% instead of GC% or NP as a feature substantially improves the predictive accuracy of the model over both GC% and NP models. However, there was no significant difference between GC% and NP models.

TABLE III

p-VALUES OF THE POST-HOC ANALYSIS FOR PHASE VARIABLE.

	ST%–GC%	ST%–NP	GC%–NP
p	0.002	< 0.001	0.094
Cohen's d	0.985	1.272	0.464

TABLE IV

ACCURACY OF ANKLE MOMENT ESTIMATION DURING WALKING.

Ref.	Method	Sens. Set	Wlk. Task	$NRMSE_{ST}$(SD)	$NRMSE_{GC}$(SD)
[12]	SA	4 pres, 1 IMU	LG	12.1%(2.2%)[a]	-
[10]	SA	2 FSRs	TM	13.5%(4.0%)	-
[13]	SA	1 FSR	TM	11.1%(4.3%)[b]	-
[20]	SS	1 IMU	TM	≥16.9%(0.9%)	-
[14]	SS	8 pres, 1 LC	TM	-	≥7.2%(-)[b]
[15]	SA	3 IMUs	TM	-	3.2%(2.1%)
Our work	**SA**	**8 FSRs, 1 IMU**	**TM**	**8.8%(1.6%)**	**3.6%(1.2%)**

[a]Estimated as the ratio between the reported RMSE and the max ankle moment range in our dataset.
[b]Estimated as the avg. reported $NRMSE_{ST}$ or $NRMSE_{GC}$ across speeds.
SA/SS: subject-agnostic/specific; LG/TM: level-ground/treadmill walking. pres: pressure sensors; LC: load cell.

V. DISCUSSION AND CONCLUSION

Combining FSR and IMU sensors and using ST% as the phase variable yielded the best results for both the ensemble GPR models ($NRMSE_{ST}$ ± SD: 8.8% ± 1.6) and the LASSO models (13.2% ± 2.5), with the former clearly outperforming the latter. These results confirm that learning-based models outperform conventional parametric regression models for ankle moment estimation.

The stance-phase ankle PDF moment is associated with the GRF and the distance between the foot COP and the ankle joint. The results in Fig. 5(b) suggest that FSRs underneath the calcaneous and the metatarsal heads can effectively capture changes in that distance and shoe size effectively [illegible] indicate that the stance-phase ankle PDF moment is more influenced by the foot acceleration than foot angular velocity, which can be explained by the correlations between the body's weight-bearing and propulsion actions, and the foot acceleration in the vertical [33] and anteroposterior [34] directions. Our findings also indicate that ST% increased the accuracy by approximately 3.5% and 3.9% compared with GC% and NP, respectively. [illegible] the temporal dynamics of the walking, thereby contributing to smaller errors relative to NP. Furthermore, because the relative duration of stance and swing phases changes across subjects and walking speeds [35], using GC% as opposed to ST% as the temporal reference is less informative. This also explains the nonsignificant improvement in accuracy between GC% and NS.

[1]The selection ratio of one feature is defined as the ratio between the number of times the feature has been selected by the GA optimizer in the LOOCV loop, and the total number of subjects (LOOCV loops).

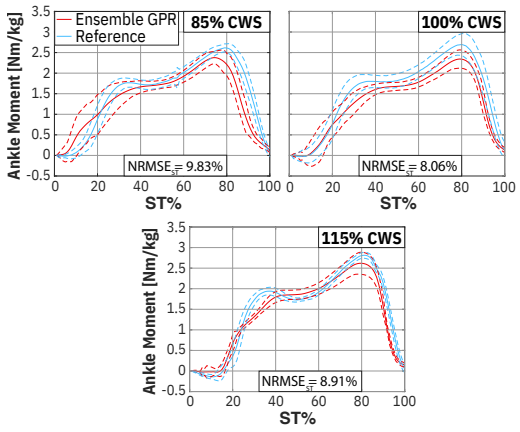

Fig. 4. Average ankle moment trajectories for a representative study participant at three walking speeds. Dashed lines indicate ±1SD.

GPR models ($NRMSE_{ST}$±SD: $8.8\% \pm 1.6$) and the LASSO models ($13.2\% \pm 2.5$), with the former clearly outperforming the latter. These results confirm that learning-based models outperforms conventional parametric regression models for ankle moment estimation. The stance-phase ankle PDF moment is associated with the GRF and the distance between the foot COP and the ankle joint. The results in Fig. 5(b) suggest that FSRs underneath the calcaneous and the metatarsal heads can effectively capture changes in that distance, and shoe size effectively reflects its maximal range. The results also indicate that the stance-phase ankle PDF moment is more influenced by foot acceleration than foot angular velocity, which can be explained by the correlations between the body's weight-bearing and propulsion actions, and the foot acceleration in the vertical [32] and anteroposterior [33] directions. Our findings also indicate that ST% increased the accuracy by approximately 3.5% and 5.9% compared with GC% and NP, respectively. A phase variable informs the models about the temporal dynamics of walking, thereby contributing to smaller errors relative to NP. Furthermore, because the relative duration of stance and swing phases changes across subjects and walking speeds [34], using GC% as opposed to ST% as the temporal reference is less informative. This also explains the nonsignificant improvement in

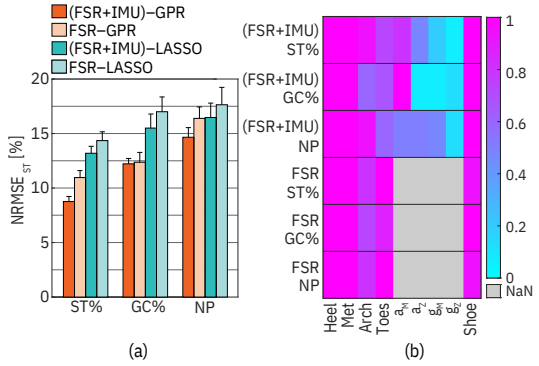

Fig. 5. **(a)** Group averages of the $NRMSE_{ST}$ for the ankle moment estimators. Error bars indicate +1SE. **(b)** Selection ratio of the input features for the optimized ensemble GPR models.

TABLE III

ACCURACY OF ANKLE MOMENT ESTIMATION DURING WALKING.

Ref.	Method	Sens. Set	Wlk. Task	$NRMSE_{ST}$(SD)	$NRMSE_{GC}$(SD)
[12]	SA	4 pres, 1 IMU	LG	12.1%(2.2%)[a]	-
[10]	SA	2 FSRs	TM	13.5%(4.0%)	-
[13]	SA	1 FSR	TM	11.1%(4.3%)[b]	-
[20]	SS	1 US	TM	≥6.9%(0.9%)	-
[14]	SS	8 pres, 1 LC	TM	-	≥7.2%(-)[b]
[15]	SA	3 IMUs	TM	-	3.2%(2.1%)
Our work	**SA**	**8 FSRs, 1 IMU**	**TM**	**8.8%(1.6%)**	**3.6%(1.2%)**

[a]Estimated as the ratio between the reported RMSE and the max ankle moment range in our dataset; [b]Estimated as the avg. reported $NRMSE_{ST}$ or $NRMSE_{GC}$ across speeds. SA/SS: subject-agnostic/specific; LG/TM: level-ground/treadmill walking. pres: pressure sensors; LC: load cell.

accuracy between GC% and NS. Individual ankle moment trajectories, shown in Fig. 4 for a representative participant, suggest that the estimator is less accurate during the first peak occurring in the early stance phase. Since this peak is linked to the contralateral foot's push-off [35], and therefore it involves dual-limb interactions, future work will need to evaluate whether the addition of bilateral sensor data may improve the model accuracy in this phase.

The accuracy of several ankle moment estimators reported in the literature is summarized in Tab. III. Because some authors reported the NRMSE normalized over the entire gait cycle ($NRMSE_{GC}$), as opposed to the stance phase ($NRMSE_{ST}$), we computed both metrics for our best-performing ensemble GPR models. These GPR models yielded smaller $NRMSE_{ST}$ than the models in [12] and [13], despite not relying on knowledge of the foot anthropometric parameters. This confirms the superior explanatory capability of learning-based models compared with simplistic biomechanical models. The GPR models also outperformed the results in [10], which nonetheless were obtained with pathological gait. In contrast to their model, which was extracted from observed correlations between FSR peaks and ankle moment peaks, the proposed GPR models take into account the changing pattern of ankle moment within the stance phase, and therefore likely more accurately reflect speed-dependent changes [2]. Although the subject-agnostic deep learning model recently presented in [15] achieved better $NRMSE_{GC}$ than our GPR models, their results were obtained using three IMUs attached to the main segments of the human leg, which require a more extensive subject setup compared with in-shoe sensors. Interestingly, the approach presented in [14] resulted in larger $NRMSE_{GC}$ compared to the proposed GPR models, despite requiring subject-specific training. This could be attributed to the different pressure sensor technology, or the absence of a sensor underneath the toes, potentially impacting the accuracy of ankle moment estimation in the late stance. The authors of [21] reported smaller $NRMSE_{ST}$, but their approach requires training a separate model at each walking speed, which may limit its applicability. Nonetheless, we note that the comparisons in Tab. III should be interpreted with caution, given the heterogeneity of sensor technologies and protocol procedures.

This study provides initial evidence that ensemble GPR models, using only in-shoe sensors, can accurately estimate ankle PDF moments during walking tasks. Study limitations include a small sample size and dependence on force-plate

data for gait segmentation. The effectiveness of the GPR models relying on ST% or GC% will be influenced by the accuracy of real-time phase estimators, thus diminishing the benefits of phase-informed models compared to simpler non-phase (NP) models. This assessment will be part of a future study implementing the proposed models on an ankle exoskeleton currently being developed in our laboratory [26].

ACKNOWLEDGMENT

This work was supported by the U.S. National Science Foundation under Grant CMMI-1944203 and by the US Department of Defense, through the Peer Reviewed Orthopaedic Research Program (PRORP), under Award No. W81XWH-22-1-0193. Opinions, interpretations, conclusions and recommendations are those of the author and are not necessarily endorsed by the US Department of Defense.

REFERENCES

[1] A. Kian, G. Widanapathirana, A. M. Joseph, D. T. Lai, and R. Begg, "Application of wearable sensors in actuation and control of powered ankle exoskeletons: A Comprehensive Review," *Sensors*, vol. 22, no. 6, p. 2244, 2022.

[2] D. A. Winter, *Biomechanics and motor control of human gait: normal, elderly and pathological*, 1991.

[3] R. Baud, A. R. Manzoori, A. Ijspeert, and M. Bouri, "Review of control strategies for lower-limb exoskeletons to assist gait," *J. Neuroeng. Rehabil.*, vol. 18, no. 1, pp. 1–34, 2021.

[4] C. Siviy, J. Bae, L. Baker, F. Porciuncula, T. Baker, T. D. Ellis, L. N. Awad, and C. J. Walsh, "Offline assistance optimization of a soft exosuit for augmenting ankle power of stroke survivors during walking," *IEEE Robot. Autom. Lett.*, vol. 5, no. 2, pp. 828–835, 2020.

[5] J. Bae, K. Kong, and M. Tomizuka, "Real-time estimation of lower extremity joint torques in normal gait," *IFAC Proceedings Volumes*, vol. 42, no. 16, pp. 443–448, 2009.

[6] E. M. McCain, T. J. Dick, T. N. Giest, R. W. Nuckols, M. D. Lewek, K. R. Saul, and G. S. Sawicki, "Mechanics and energetics of post-stroke walking aided by a powered ankle exoskeleton with speed-adaptive myoelectric control," *J. Neuroeng. Rehabil.*, vol. 16, no. 1, pp. 1–12, 2019.

[7] F. Tamburella, N. Tagliamonte, I. Pisotta, M. Masciullo, M. Arquilla, E. Van Asseldonk, H. Van der Kooij, A. Wu, F. Dzeladini, A. Ijspeert *et al.*, "Neuromuscular controller embedded in a powered ankle exoskeleton: Effects on gait, clinical features and subjective perspective of incomplete spinal cord injured subjects," *IEEE Trans. Neural Syst. Rehabil. Eng.*, vol. 28, no. 5, pp. 1157–1167, 2020.

[8] T. Xue, Z. Wang, T. Zhang, and M. Zhang, "Adaptive oscillator-based robust control for flexible hip assistive exoskeleton," *IEEE Robot. Autom. Lett.*, vol. 4, no. 4, pp. 3318–3323, 2019.

[9] V. Arnez-Paniagua, W. Huo, I. Colorado-Cervantes, S. Mohammed, and Y. Amirat, "A hybrid approach towards assisting ankle joint of paretic patients," *IFES Hybrid approaches to FES*, vol. 4, 2016.

[10] G. M. Gasparri, J. Luque, and Z. F. Lerner, "Proportional joint-moment control for instantaneously adaptive ankle exoskeleton assistance," *IEEE Trans. Neural Syst. Rehabil. Eng.*, vol. 27, no. 4, 2019.

[11] M. Jeong, H. Woo, and K. Kong, "A study on weight support and balance control method for assisting squat movement with a wearable robot, angel-suit," *Int J Control Autom Syst*, vol. 18, 2020.

[12] H. Choi, K. Kim, P.-G. Jung, B. Na, D.-w. Rha, K. Jung, and K. Kong, "Ankle joint moment estimation based on smart shoes," *IFAC-PapersOnLine*, vol. 50, no. 1, pp. 1366–1371, 2017.

[13] S. S. P. A. Bishe, T. Nguyen, Y. Fang, and Z. F. Lerner, "Adaptive ankle exoskeleton control: Validation across diverse walking conditions," *IEEE Trans. Med. Robot. Bionics*, vol. 3, no. 3, pp. 801–812, 2021.

[14] D. A. Jacobs and D. P. Ferris, "Estimation of ground reaction forces and ankle moment with multiple, low-cost sensors," *J. Neuroeng. Rehabil.*, vol. 12, no. 1, pp. 1–12, 2015.

[15] M. S. B. Hossain, Z. Guo, and H. Choi, "Estimation of Lower Extremity Joint Moments and 3D Ground Reaction Forces Using IMU Sensors in Multiple Walking Conditions: A Deep Learning Approach," *IEEE J Biomed Health Inform*, 2023.

[16] M. M. Ardestani, X. Zhang, L. Wang, Q. Lian, Y. Liu, J. He, D. Li, and Z. Jin, "Human lower extremity joint moment prediction: A wavelet neural network approach," *Expert Syst. Appl.*, vol. 41, no. 9, 2014.

[17] B. Xiong, N. Zeng, H. Li, Y. Yang, Y. Li, M. Huang, W. Shi, M. Du, and Y. Zhang, "Intelligent prediction of human lower extremity joint moment: An artificial neural network approach," *IEEE Access*, vol. 7, pp. 29 973–29 980, 2019.

[18] E. Grzesiak, J. Sloboda, and H. C. Siu, "Predicting ankle moment trajectory with adaptive weighted ensemble of LSTM networks," in *2022 IEEE High Perform. Extreme Comput. Conf. (HPEC)*. IEEE, 2022, pp. 1–7.

[19] J. Sloboda, P. Stegall, R. J. McKindles, L. Stirling, and H. C. Siu, "Utility of inter-subject transfer learning for wearable-sensor-based joint torque prediction models," in *2021 43rd Annu. Int. Conf. IEEE Eng. Med. Biol. Soc. (EMBC)*. IEEE, 2021, pp. 4901–4907.

[20] K. G. Rabe, M. H. Jahanandish, K. Hoyt, and N. P. Fey, "Use of sonomyography for continuous estimation of hip, knee and ankle moments during multiple ambulation tasks," in *2020 8th IEEE RAS/EMBS Int. Conf. Biomed. Robot. Biomechatronics (BioRob)*. IEEE, 2020.

[21] Q. Zhang, N. Fragnito, X. Bao, and N. Sharma, "A deep learning method to predict ankle joint moment during walking at different speeds with ultrasound imaging: A framework for assistive devices control," *Wearable Technologies*, vol. 3, p. e20, 2022.

[22] T. T. H. Duong, D. Uher, S. D. Young, T. Duong, M. Sangco, K. Cornett, J. Montes, and D. Zanotto, "Gaussian Process Regression for COP Trajectory Estimation in Healthy and Pathological Gait Using Instrumented Insoles," in *2021 IEEE/RSJ Int. Conf. Intell. Robots Syst. (IROS)*, 2021, pp. 9548–9553.

[23] T. T. H. Duong, D. Uher, J. Montes, and D. Zanotto, "Ecological Validation of Machine Learning Models for Spatiotemporal Gait Analysis in Free-Living Environments Using Instrumented Insoles," *IEEE Robot. Autom. Lett.*, vol. 7, no. 4, pp. 10 834–10 841, 2022.

[24] T. T. H. Duong, D. Uher, S. D. Young, R. Farooquee, A. Druffner, A. Pasternak, C. Kanner, M. Fragala-Pinkham, J. Montes, and D. Zanotto, "Accurate COP Trajectory Estimation in Healthy and Pathological Gait Using Multimodal Instrumented Insoles and Deep Learning Models," *IEEE Trans. Neural Syst. Rehabil. Eng.*, vol. 31, 2023.

[25] B. A. Gebre, R. Nogueira, S. Patidar, R. Belle-Isle, K. Nolan, K. Pochiraju, and D. Zanotto, "Efficient digital modeling and fabrication workflow for individualized ankle exoskeletons," in *ASME Int Mech Eng Congress Expo*, vol. 85598. American Society of Mechanical Engineers, 2021, p. V005T05A068.

[26] M. Eraky, A. Li, M. H. Rocha, A. Teker, B. Gebre, K. J. Nolan, K. Pochiraju, and D. Zanotto, "A Novel Personalized Ankle Exoskeleton with Co-Located SEA for Gait Training," in *2024 10th IEEE RAS/EMBS Int. Conf. Biomed. Robot. Biomechatronics (BioRob)*, 2024.

[27] U. Dal, T. Erdogan, B. Resitoglu, and H. Beydagi, "Determination of preferred walking speed on treadmill may lead to high oxygen cost on treadmill walking," *Gait & posture*, vol. 31, no. 3, 2010.

[28] H. Zhang, Y. Guo, and D. Zanotto, "Accurate ambulatory gait analysis in walking and running using machine learning models," *IEEE Trans. Neural Syst. Rehabil. Eng.*, vol. 28, no. 1, pp. 191–202, 2019.

[29] S. L. Delp, F. C. Anderson, A. S. Arnold, P. Loan, A. Habib, C. T. John, E. Guendelman, and D. G. Thelen, "Opensim: open-source software to create and analyze dynamic simulations of movement," *IEEE. Trans. Biomed. Eng.*, vol. 54, no. 11, pp. 1940–1950, 2007.

[30] N. Jorge and J. W. Stephen, *Numerical optimization*. Spinger, 2006.

[31] C. E. Rasmussen and C. K. I. Williams, *Gaussian Processes for Machine Learning*. The MIT Press, 11 2005.

[32] D. P. Raper, J. Witchalls, E. J. Philips, E. Knight, M. K. Drew, and G. Waddington, "Use of a tibial accelerometer to measure ground reaction force in running: A reliability and validity comparison with force plates," *J Sci Med Sport*, vol. 21, no. 1, pp. 84–88, 2018.

[33] K. J.-H. Ngoh, D. Gouwanda, A. A. Gopalai, and Y. Z. Chong, "Estimation of vertical ground reaction force during running using neural network model and uniaxial accelerometer," *J. Biomech.*, vol. 76, pp. 269–273, 2018.

[34] F. Hebenstreit, A. Leibold, S. Krinner, G. Welsch, M. Lochmann, and B. M. Eskofier, "Effect of walking speed on gait sub phase durations," *Hum. Mov. Sci.*, vol. 43, pp. 118–124, 2015.

[35] A. Karatsidis, G. Bellusci, H. M. Schepers, M. De Zee, M. S. Andersen, and P. H. Veltink, "Estimation of ground reaction forces and moments during gait using only inertial motion capture," *Sensors*, vol. 17, no. 1, p. 75, 2016.